Supporting Information For

A Dinuclear Rh(-I)/Rh(I) Complex Bridged by Biphilic Phosphinine Ligands

Koichiro Masada, Kiyosumi Okabe, Shuhei Kusumoto, and Kyoko Nozaki*

Department of Chemistry and Biotechnology, Graduate School of Engineering, The University of Tokyo, 7-3-1 Hongo, Bunkyo-ku, Tokyo 113-8656, Japan.

Contents: **page**

I. Experimental Procedures

I-I. General

Manipulation: Unless otherwise noted, all manipulations were carried out in a glovebox filled with argon gas or with standard Schlenk techniques under nitrogen gas purified by passing through Nikka Seiko dry column DC-L4 (NIKKA SEIKO Co., LTD). Air- and moisture-sensitive liquids and solutions were transferred via a syringe or a stainless or a PTFE cannula. All manipulations with heating were carried out using an oil bath.

Instrumentation: Nuclear magnetic resonance (NMR) spectra were recorded on BRUKER Ascend500 spectrometer (^{1}H: 500 MHz, ^{13}C: 126 MHz, ^{31}P NMR: 202 MHz with digital resolution of 0.305, 0.908, 4.40 Hz respectively) at ambient temperature. Chemical shift values for protons were referenced to the residual proton resonance of THF-d_8 (C_4D_8O, δ: 3.58). Chemical shift values for ^{13}C nuclei were referenced to the carbon resonance of THF-d_8 (δ: 67.21). Mass spectra (MS) were taken with an electron spray ionization time-of-flight (ESI-TOF) method on a JEOL JMS-T100LP AccuTOF LC-plus mass spectrometer. Infrared (IR) spectra were recorded on a JASCO FTIR-6600 equipped with an attenuated total reflection (ATR) system. Ultraviolet/Visible (UV/Vis) absorption spectra were recorded on a Shimadzu UV-3100 spectrometer. X-ray crystallographic analyses were performed on a Rigaku Varimax with hybrid photon counting detector. XPS measurements were performed on a PHI5000 VersaProbe.

Materials: Anhydrous diethyl ether, hexane, tetrahydrofuran (THF), and toluene were purchased from Kanto Chemical Co. Inc. (Kanto) and purified by the method of Pangborn et al.[1] THF-d_8 (purchased from Kanto) were dried over MS4A. The following reagents were purchased and used as received: (1,5-cyclooctadiene)rhodium chloride dimer ($[RhCl(cod)]_2$, Tokyo Chemical Industry Co., Ltd., TCI), napthalene (Kanto), sodium metal (Kanto). 2,6-bis(2'-diphenylphosphinophenyl)-4-phenylphosphinine (**1**)[2] and $[K(18\text{-crown-}6)][Rh(CO)(PPh_3)_3]$[3] were prepared following the literature procedure.

I-II. Synthesis and Characterization of the Novel Compounds

Neutral dirhodium complex (2)

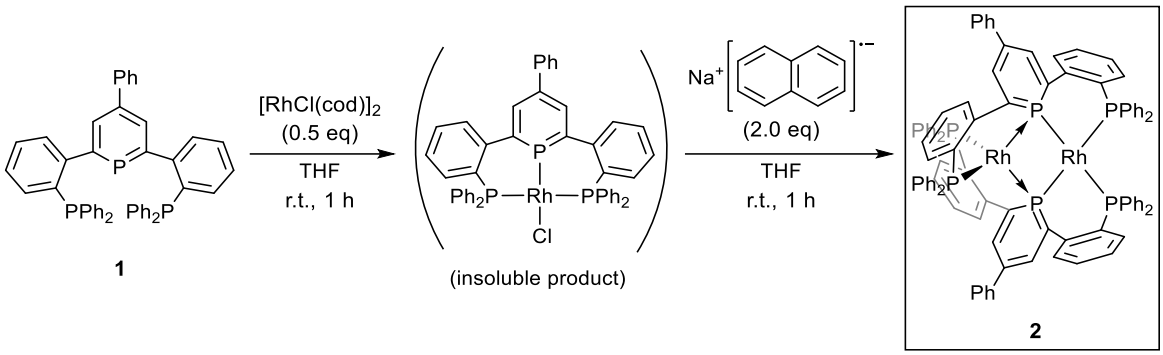

In an oven-dried 15 mL screw-capped glass vial, phosphinine pincer ligand **1** (44.0 mg, 63.5 µmol) and (1,5-cyclooctadiene)rhodium chloride dimer ($[RhCl(cod)]_2$, 15.7 mg, 31.8 µmol) were dissolved in THF (2 mL) and the mixture was stirred for one hour to give orange suspension. The precipitates were collected by filtration and washed with THF (1 mL x 2) followed by pentane (1 mL x 3). The solid was dried under reduced pressure to obtain orange powder (53.6 mg). The compound was hardly soluble in common solvents, and the product was used without further purification. See the next section for in situ NMR spectra of the Rh chloride species.

Note: In the following manipulation, THF was dried over sodium-potassium alloy (NaK) and passed through a pad of dry silica gel before use.

In an oven-dried 15 mL screw-capped glass vial, metallic Na (12.6 mg, 0.548 mmol, 8.63 equiv vs ligand **1**) and naphthalene (16.6 mg, 0.130 mmol, 2.05 equiv vs ligand **1**) was dissolved in THF (5 mL). After stirring the purple solution for one hour, the solution was decanted into another oven-dried 15 mL screw-capped glass vial to remove the residual Na metal. To this solution was added rhodium complex (53.6 mg, prepared from 63.5 µmol of ligand **1**) obtained by the procedure above and the mixture was stirred for another one hour to afford dark-green solution. After filtration using a PTFE syringe filter, pentane was layered on the filtrate. The solution was stored at −25°C overnight to afford dark green crystals. The crystals were washed with pentane (1 mL x 3) and dried *in vacuo* to afford compound **2** as dark-green powder (21.9 mg, 13.8 µmol, 43 %, 2 steps). The crystals suitable for the X-ray crystallographic analysis were obtained by allowing the vapor of pentane to diffuse into toluene solution of complex **2**. Because compound **2** shows complicated NMR spectra in concentrated media, probably due to aggregation as mentioned in the main text, the low concentration of the solution for characterization made it difficult to observe all the ^{13}C signals. The ^{31}P NMR spectra in varied concentrations were shown in Figure S6.

IR (ATR): 3047, 1596, 1558, 1477, 1453, 1434, 1342, 1285, 1182, 1119, 1092, 1065, 1028, 841, 741, 694 cm^{-1}.

^1H NMR (500 MHz, THF-d_8) δ 7.26 (t, J = 8.4 Hz, 8H), 7.15–6.92 (m, 46H), 6.80–6.71 (m, 8H), 6.56–6.47 (m, 8H).

^{13}C NMR (126 MHz, THF-d_8) δ 148.7, 144.7, 140.7, 137.6, 137.0, 136.7, 135.9 (d, J_{CP} = 15 Hz), 135.8, 135.6, 132.8, 130.4, 130.1, 129.7, 129.2, 129.0, 129.0, 128.6, 127.9 (d, J_{CP} = 8 Hz), 127.5 (d, J_{CP} = 9 Hz), 126.3, 126.1, 125.2.

^{31}P NMR (202 MHz, THF-d_8) δ 197.8–195.9 (m), 39.8–37.6 (m).

HRMS (ESI) *m/z* calcd for $C_{94}H_{69}P_6Rh_2$ $[M-H]^+$: 1589.19296; found: 1589.18912.

Dianionic dirhodium complex (3)

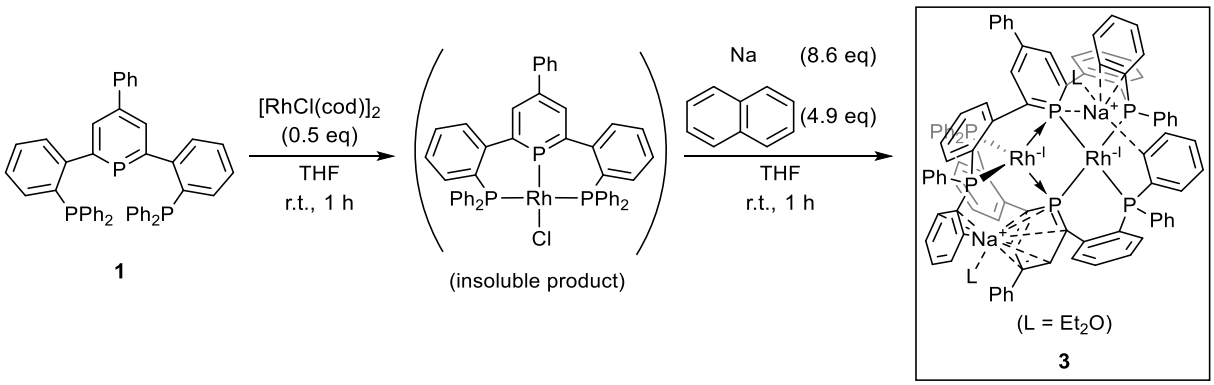

In an oven-dried 15 mL screw-capped glass vial, phosphinine pincer ligand **1** (11.7 mg, 16.9 μmol) and (1,5-cyclooctadiene)rhodium chloride dimer ($[RhCl(cod)]_2$, 4.2 mg, 8.3 μmol) were dissolved in toluene (1.5 mL) and the mixture was stirred for one hour to give orange suspension. The precipitates were collected by filtration and washed with hexane (1 mL x 3). The solid was dried under reduced pressure to obtain orange powder (12.9 mg). The compound was hardly soluble in common solvents, and the product was used without further purification.

Note: In the following manipulation, THF was dried over sodium-potassium alloy (NaK) and passed through a pad of dry silica gel before use.

In an oven-dried 15 mL screw-capped glass vial, metallic Na (8.2 mg, 0.36 mmol, 8.63 equiv vs $[RhCl(cod)]_2$) and naphthalene (5.2 mg, 40.6 μmol, 4.9 equiv vs $[RhCl(cod)]_2$) were dissolved in THF (5 mL). After stirring the purple solution for one hour, rhodium complex (12.9 mg, prepared from 8.3 μmol of $[RhCl(cod)]_2$) obtained by the procedure above and the mixture was stirred for another one hour. The volatiles were removed under reduced pressure and the residue was dissolved in Et_2O. The crystals appropriate for single-crystal X-ray analysis was obtained by layering pentane to this solution.

The product was too unstable to fully characterize by spectroscopic methods and determine the yield.

I-III. *In Situ* NMR Spectra of the Rhodium Chloride Species

In a J-young-capped NMR tube, phosphinine pincer ligand **1** (3.9 mg, 5.6 µmol) and (1,5-cyclooctadiene)rhodium chloride dimer ($[RhCl(cod)]_2$, 1.4 mg, 2.8 µmol) were dissolved in THF-d_8 (0.6 mL). ^{31}P NMR (Figure S1) and ^{1}H NMR (Figure S2) spectra of this mixture was measured within 10 minutes.

The chemical shifts and the coupling patterns are similar to the previously reported complex **S1** shown below,[4] which suggests the formation of Ph analogue **S2**, its oligomer, or its polymer.

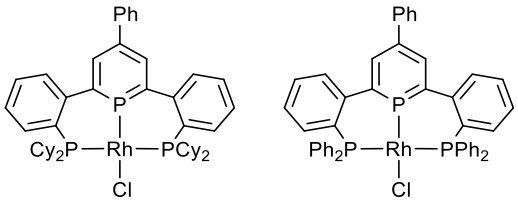

S1 **S2**

With prolonged reaction time, insoluble orange powder was formed in the reaction mixture that made the further analysis difficult.

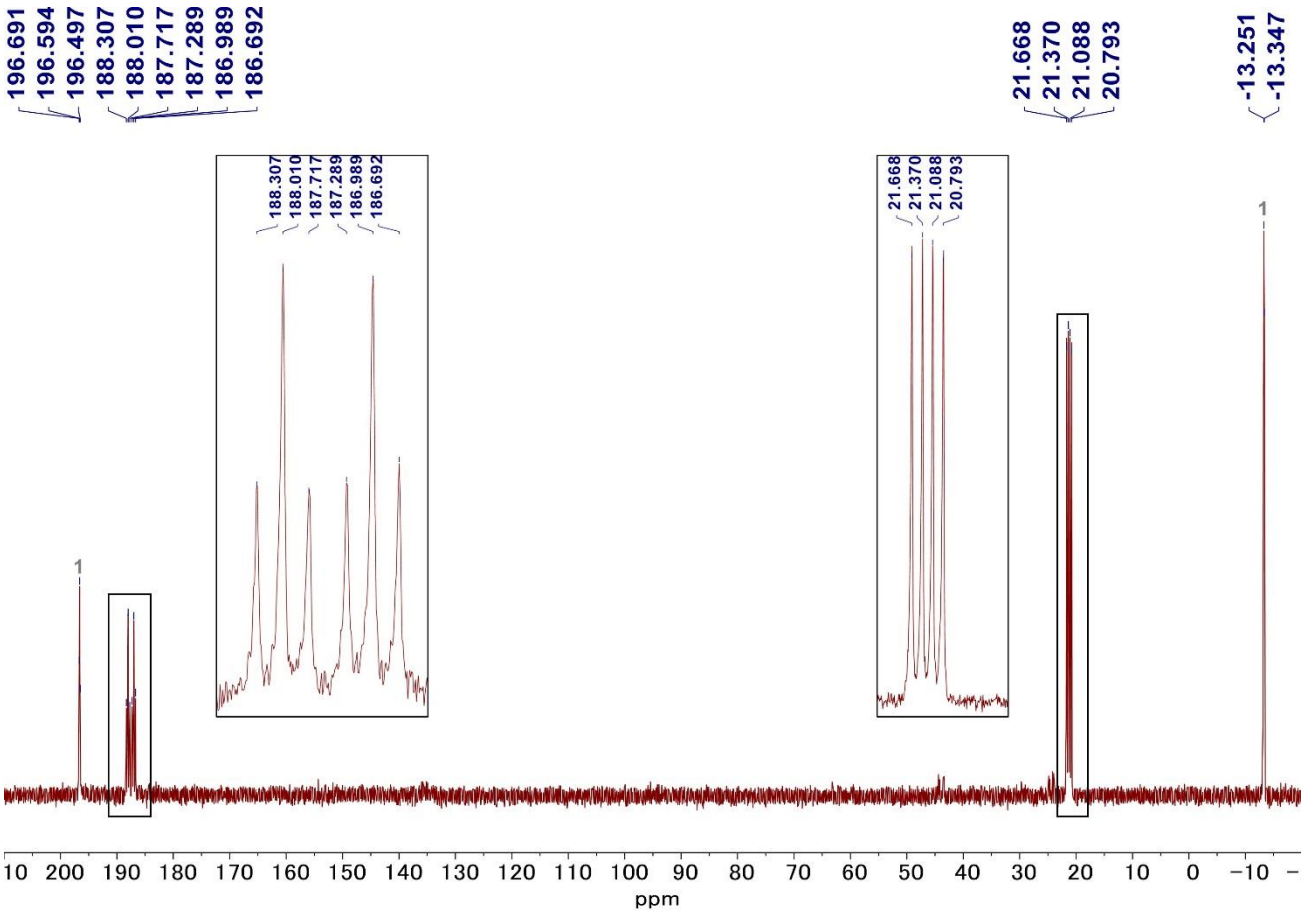

Figure S1. ^{31}P NMR spectrum of the mixture and ligand **1** and $[RhCl(cod)]_2$ (202 MHz, THF-d_8).

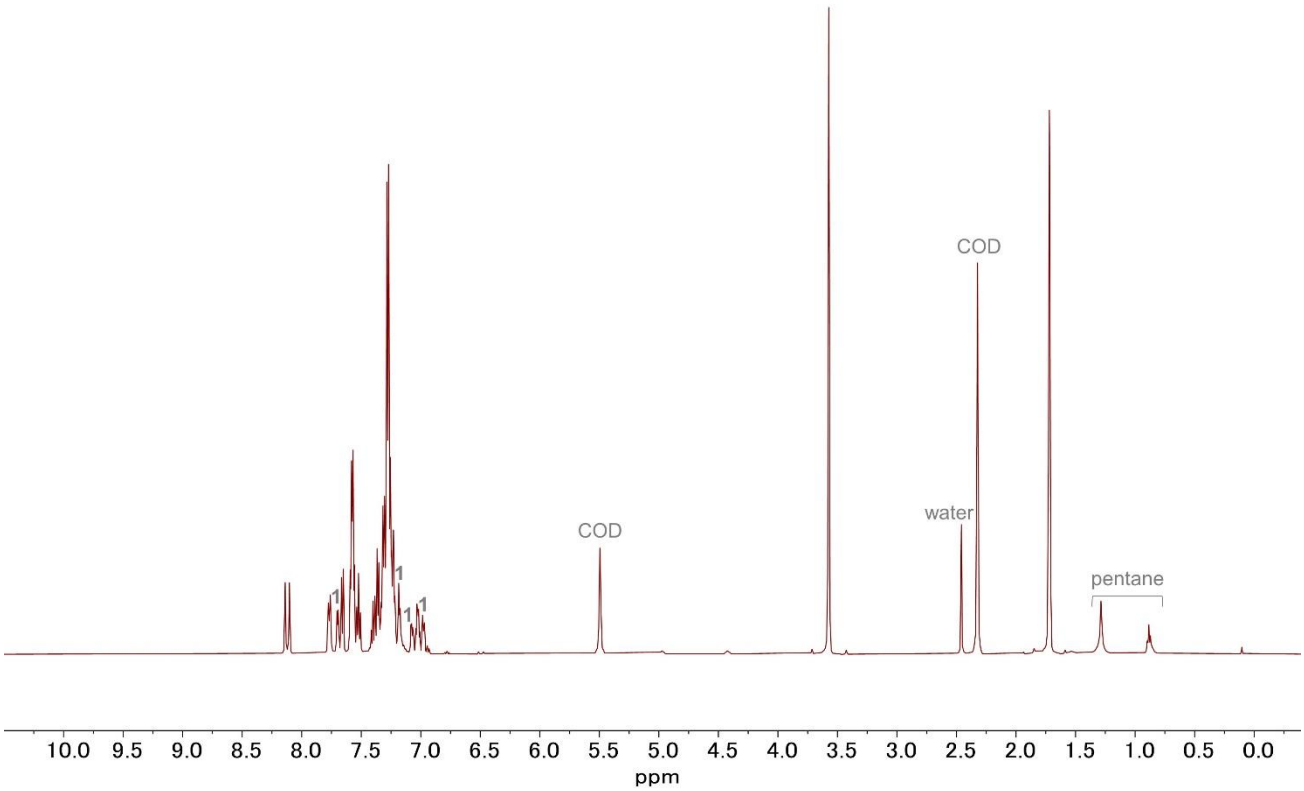

Figure S2. ^{1}H NMR spectrum of the mixture and ligand **1** and $[RhCl(cod)]_2$ (500 MHz, THF-d_8).

II. NMR Spectra of Neutral Dirhodium Complex 3

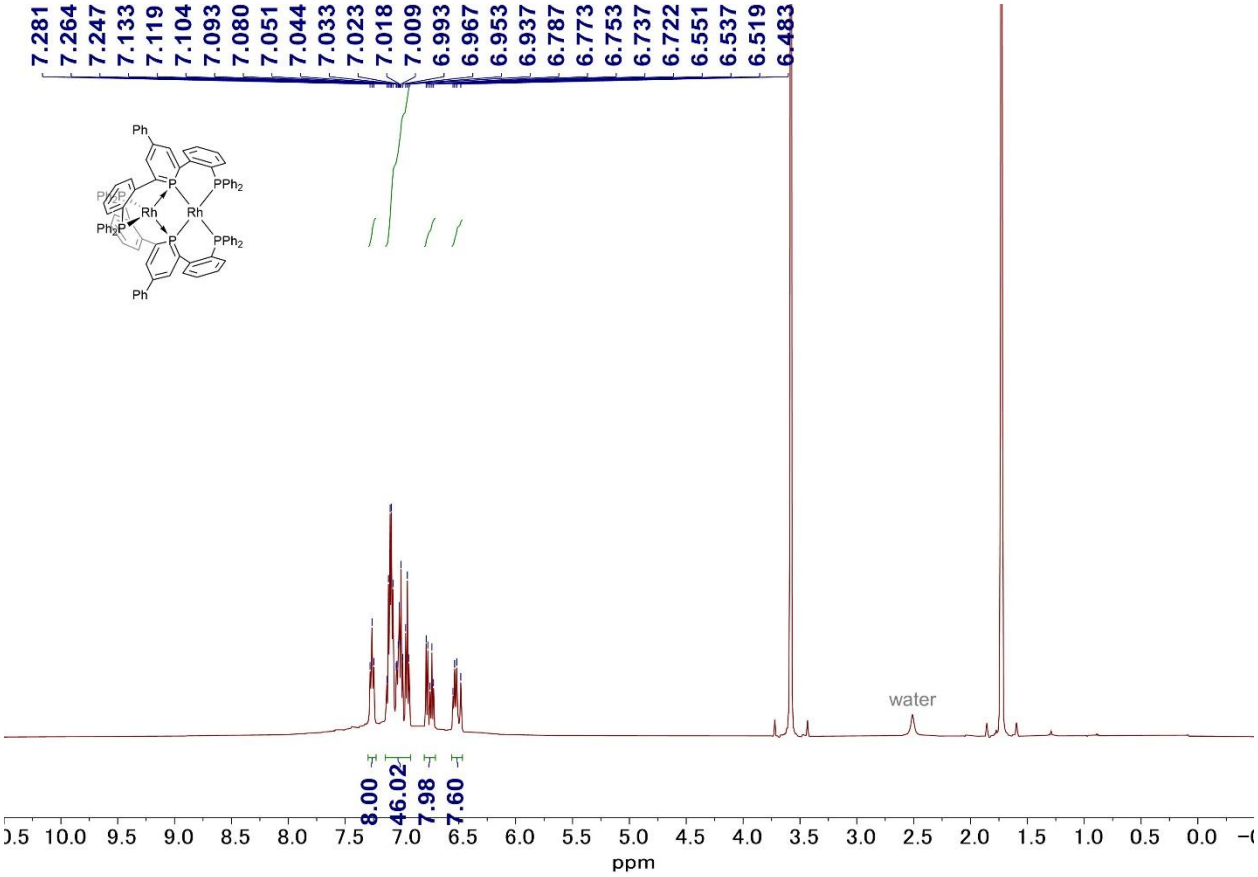

Figure S3. ^{1}H NMR spectrum of complex **2** (500 MHz, THF-d_8)

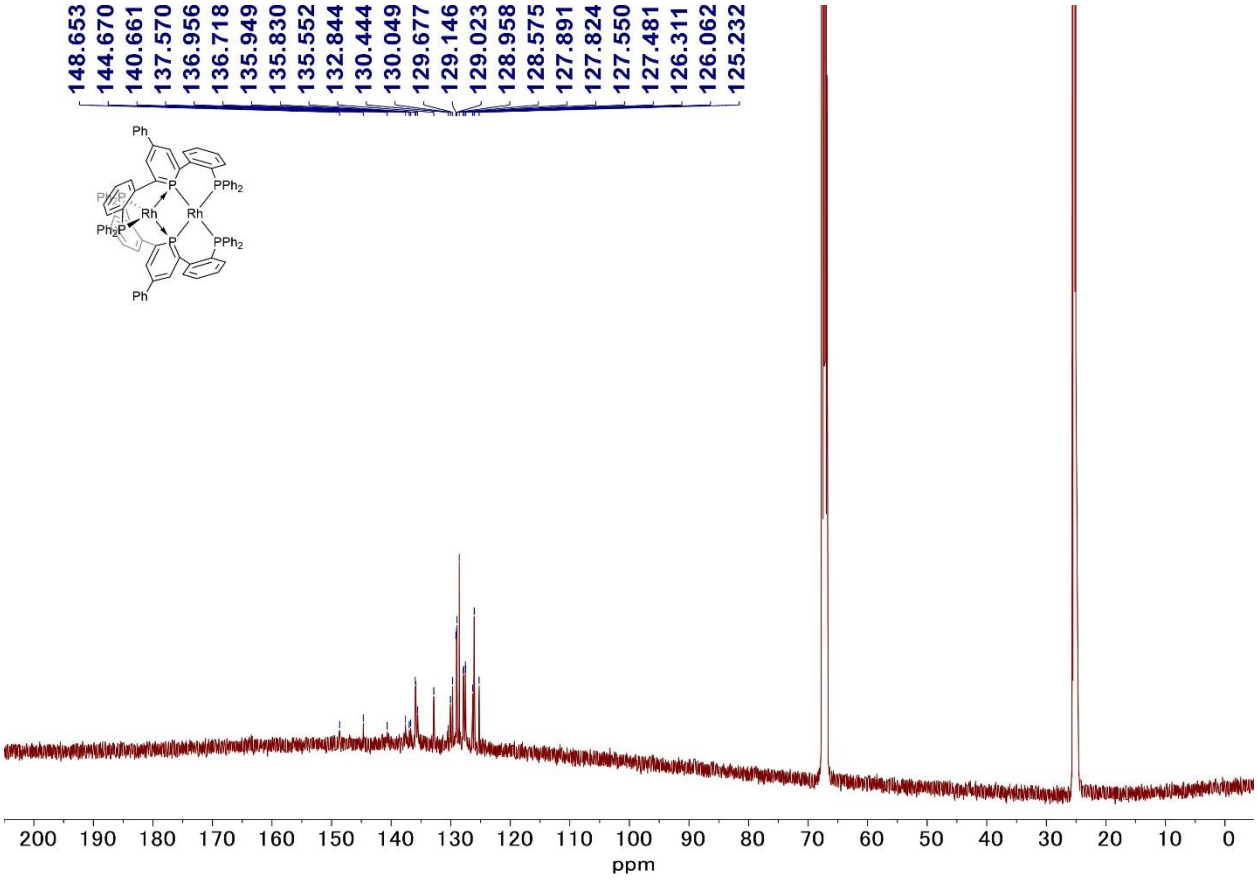

Figure S4. ^{13}C NMR spectrum of complex **2** (126 MHz, THF-d_8)

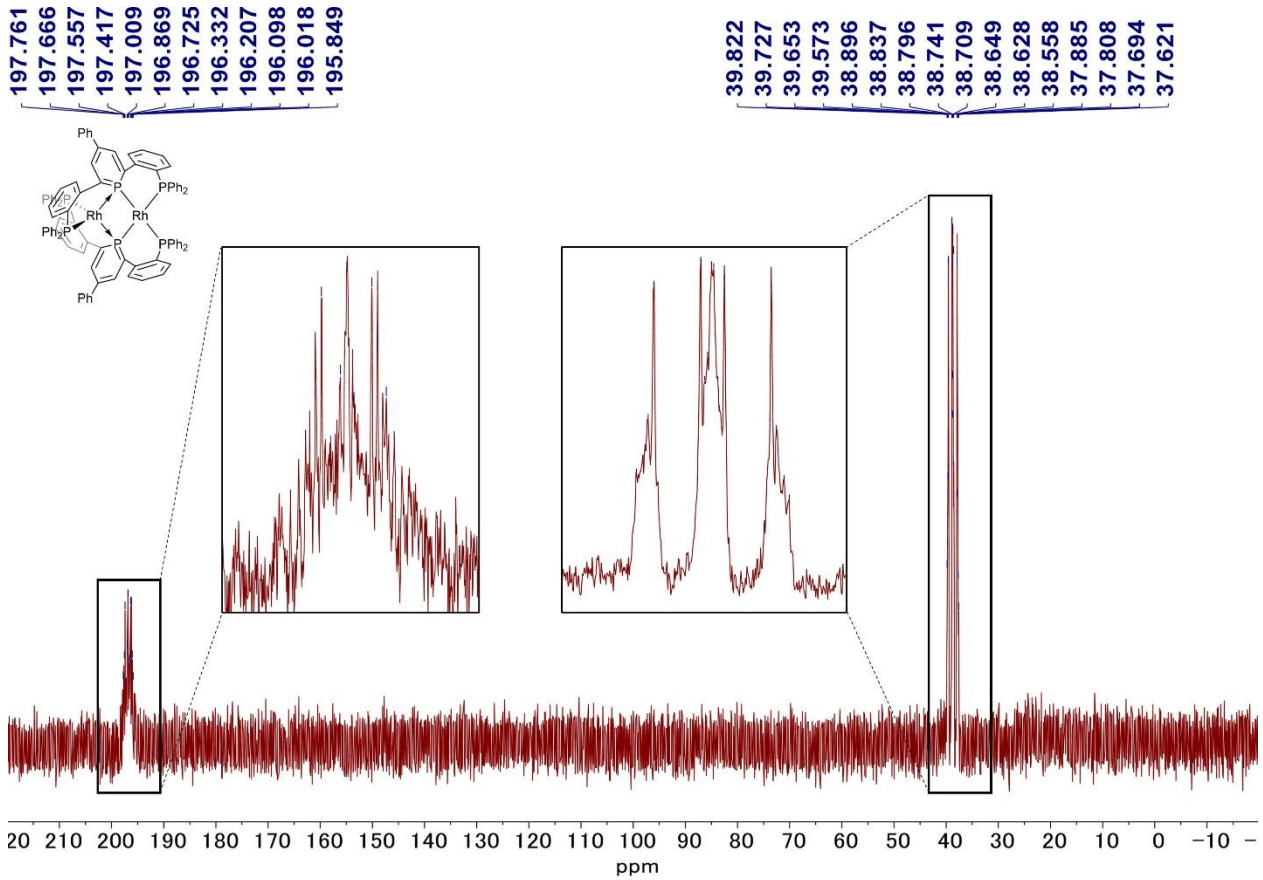

Figure S5. ^{31}P NMR spectrum of complex **2** (202 MHz, THF-d_8)

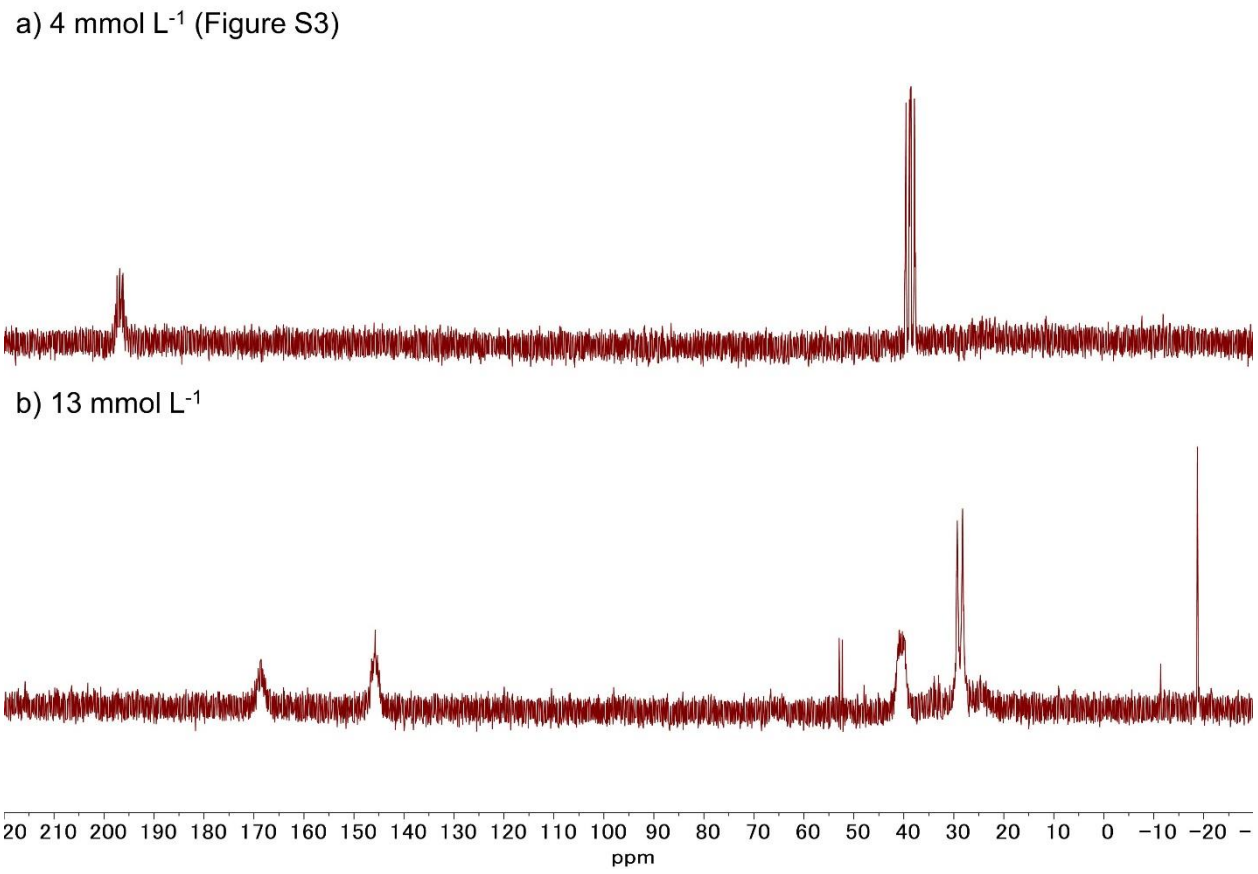

Figure S6. ^{31}P NMR spectrum of complex **2** with varied concentrations (202 MHz, THF-d_8)

III. IR spectra of Neutral Dirhodium Complex 2

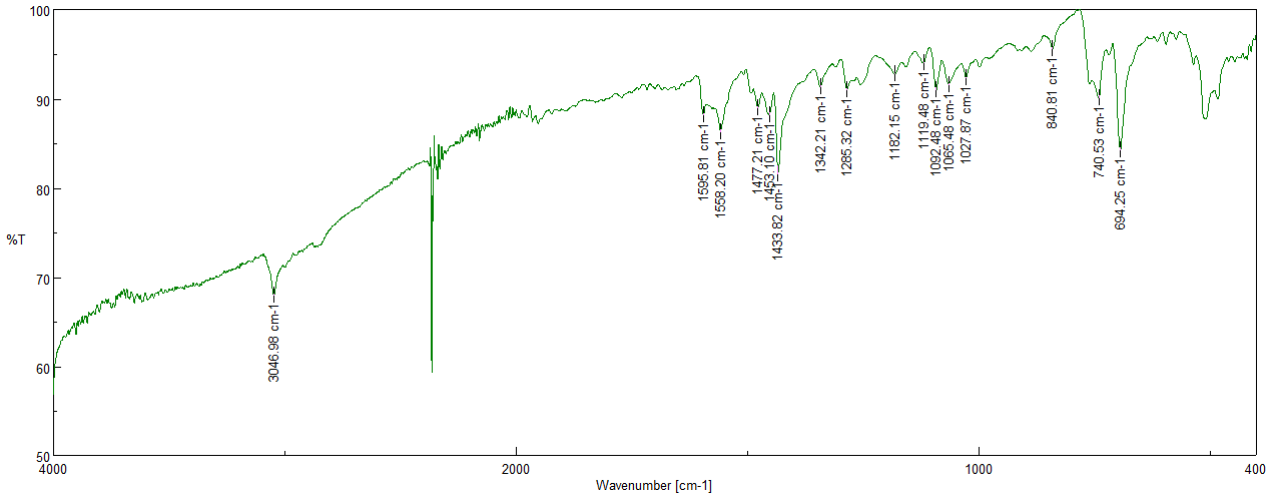

Figure S7. IR spectrum of compound **2** (ATR)

IV. Detail of the X-ray Crystallographic Analyses

Details of the crystal data and a summary of the intensity data collection parameters are listed in Table S1. X-ray crystallographic analyses of single crystals were performed on a Rigaku VariMax with Hybrid Photon Counting Detector. A single crystal was mounted with mineral oil on a loop-type mount and transferred to the goniometer. The radiation was performed with graphite monochromated Mo Kα (λ = 0.71075 Å) at 50 kV and 24 mA for all the compounds. All the following procedure for analysis, Olex2[5] was used as a graphical interface. The structure was solved by direct methods with (SHELXT-2018/2)[6] and refined by full-matrix least-squares techniques against F^2 (SHELXL-2017/1).[7] The intensities were corrected for Lorentz and polarization effects. The non-hydrogen atoms were refined anisotropically. Hydrogen atoms were placed using AFIX instructions. The resulting CIF files are also attached as supporting information.

Table S1. Crystallographic data and structure refinement details for compounds **2**, and **3**

		2	**3**
CCDC number		2260653	2260654
Molecular formula		$C_{101}H_{78}P_6Rh_2$	$C_{102}H_{90}Na_2O_2P_6Rh_2$
Formula weight		1683.27	1785.35
Temperature (K)		93(2)	93(2)
Wavelength (Å)		0.71073	0.71073
Crystal system		monoclinic	triclinic
Space group		$P2_1/c$	P-1
Unit cell dimensions	a (Å)	16.4813(3)	13.1385(2)
	b (Å)	19.1877(3)	16.5943(2)
	c (Å)	28.5841(5)	20.8960(3)
	α (°)	90	93.6980(10)
	β (°)	95.453(2)	91.5350(10)
	γ (°)	90	98.4790(10)
Volume (Å^3)		8998.5(3)	4493.61(11)
Z		4	2
Density (calculated) (mg·m^{-3})		1.242	1.319
Absorption coefficient (mm^{-1})		0.518	0.533
F(000)		3456.0	1840.0
Theta range (°)		2.24–29.54	2.106–32.651
Index ranges		-21 ≤ h ≤ 21	-19 ≤ h ≤ 19
		-23 ≤ k ≤ 26	-24 ≤ k ≤ 24
		-38 ≤ l ≤ 37	-31 ≤ l ≤ 28
Reflections collected		128571	228372
Independent reflections		22289	30654
R(int)		0.0415	0.0514
Data / restraints / parameters		22289/0/983	30654/109/1031
Goodness-of-fit on F^2		1.114	1.030
Final R indices [I>2σ(I)]	R_1	0.0494	0.0739
	wR_2	0.1338	0.1955
R indices (all data)	R_1	0.0563	0.0916
	wR_2	0.1401	0.2075
Largest diff. peak and hole (e·Å^3)		1.49/-0.87	2.49/-1.65

V. Detail of XPS Measurements

The XPS measurements were performed on a PHI5000 VersaProbe using aluminium Kα radiation (*hv* = 1486.6 eV, 15 kV, 1.7 mA). Samples are mounted on carbon tapes in a glovebox filled with argon gas. Samples were introduced to the XPS chamber using a specified transfer vessel for keeping samples under an inert atmosphere. One set of experiments was performed with the charge neutralizer.

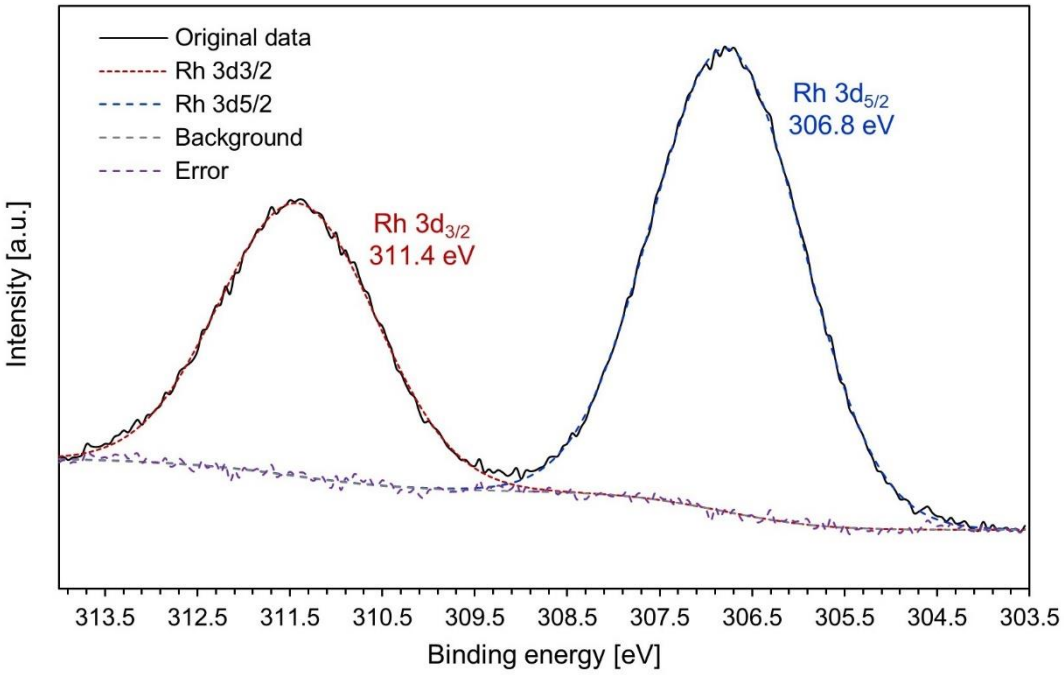

Figure S8. An XPS spectrum of [K(18-crown-6)][Rh(CO)(PPh_3)$_3$]. The continuous black line indicates the original spectrum; the blue and red dashed lines indicate the deconvoluted signals; the purple dashed line is the error of the deconvoluted signals from the original spectrum; the grey dashed line is the background signals.

VI. Methods and Discussions for Theoretical Calculations

DFT calculations were performed using the Gaussian 16 Program, revision C.02[8] All geometry optimizations followed by frequency calculations were performed using PBE0[9] level with Karlsruhe split valence polarization basis set (def2-SVP)[10,11] in gas phase. Dispersion effects were treated in the Grimme's DFT-D3 framework.[12] The transition state was calculated at the same calculation level. Each molecular orbital was calculated using the optimized structures. Single point energy calculations were performed using ωB97X-D[13] functional and Karlsruhe valence triple-zeta polarization basis sets (def2-TZVP).[10,11]

VI-I. NBO Analysis of Complex 2

NBO analyses were conducted with NBO 6.0 at PBE0 level with Karlsruhe valence triple-zeta polarization basis sets (def2-TZVP). Dispersion effects were treated in the Grimme's DFT-D3 framework.

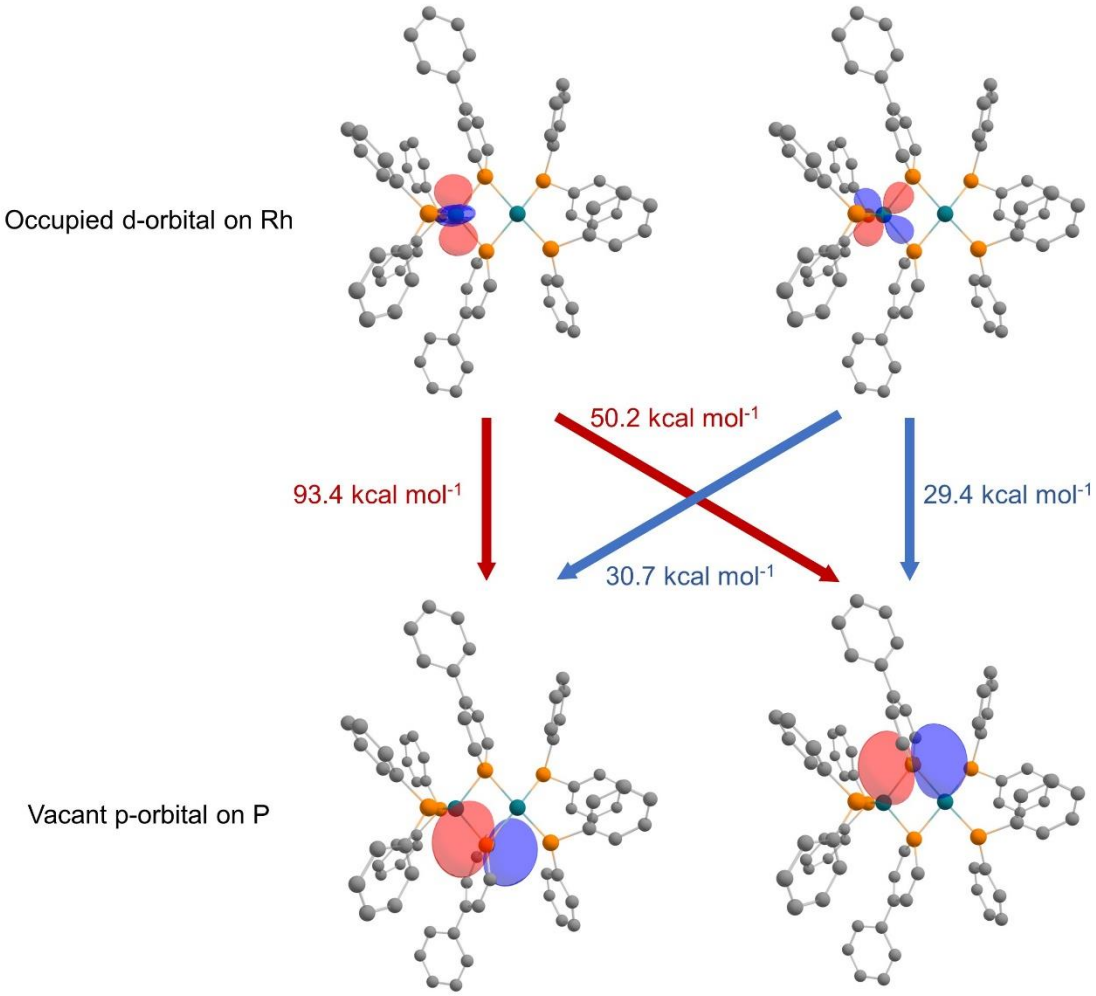

Figure S9. Back-donation energies calculated by NBO second order perturbation theory analysis.

VI-II. TD-DFT Calculation of Complex 2

TD-DFT calculation was performed using PBE0 level and Karlsruhe valence triple-zeta polarization basis sets (def2-TZVP) with PCM solvation in THF. Dispersion effects were treated in the Grimme's DFT-D3 framework.

Table S2. Major transitions of complex **2** by TD-DFT at the PBE0-D3/ def2-TZVP level (in THF)

Wavelength [nm]	**oscillator strength [*f*]**	**major contributions**
615.45	0.2548	HOMO−2 → LUMO (0.55226) HOMO → LUMO (−0.40913)
670.73	0.1999	HOMO → LUMO (0.56281) HOMO−2 → LUMO (0.40211) HOMO−2 → LUMO+1 (−0.10388)
557.42	0.0478	HOMO → LUMO+1 (0.68585)
426.77	0.0441	HOMO → LUMO+4 (0.45262) HOMO−3 → LUMO+1 (−0.41377) HOMO−1 → LUMO+2 (0.19085) HOMO → LUMO+3 (−0.14951) HOMO → LUMO+8 (−0.11106)
440.98	0.0374	HOMO−4 → LUMO (0.64641) HOMO−4 → LUMO+1 (0.22478)

VI-III. Computed Structure of Complex 3

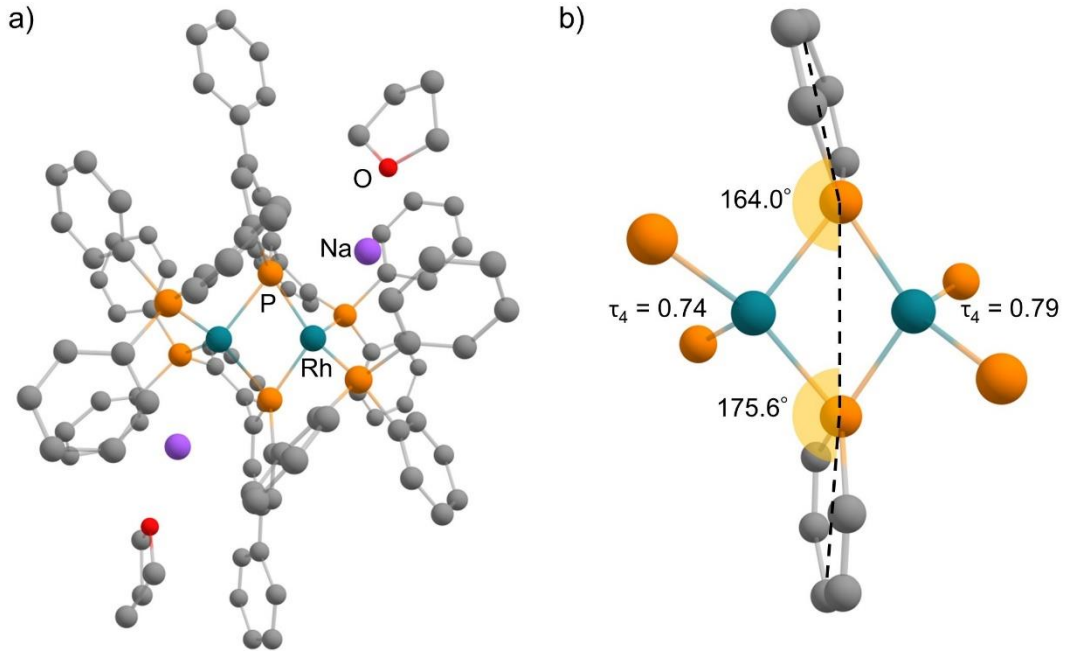

Figure S10. Computed structure of complex **3** with the contacting Na cations (Et_2O molecules are substituted by THF molecules for the ease of calculations).

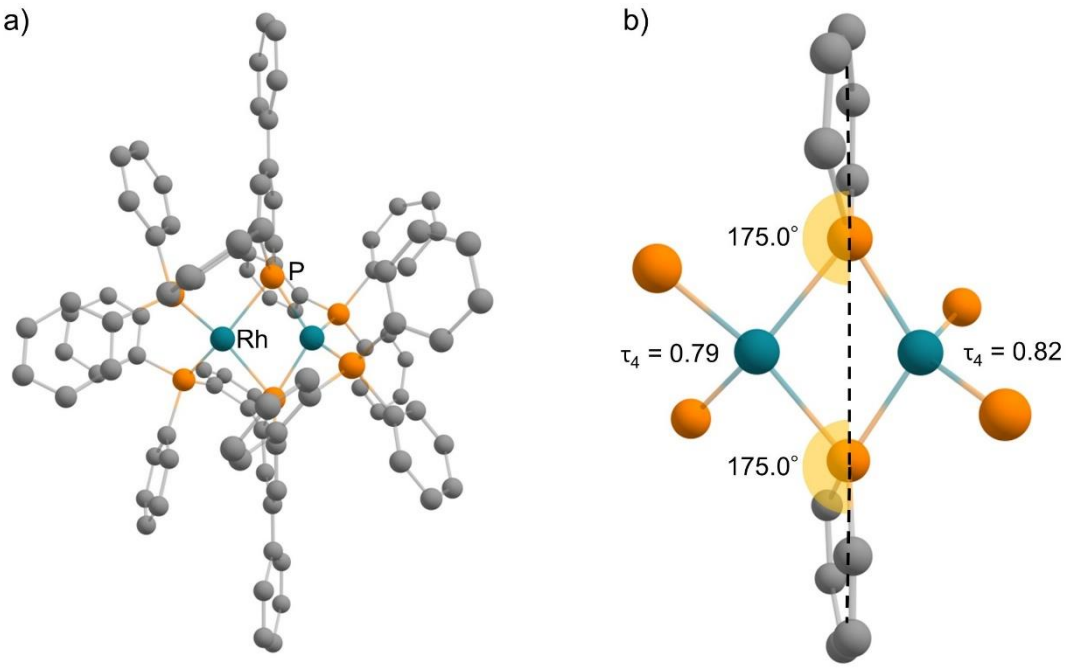

Figure S11. Computed structure of complex **3** without the contacting Na cations.

VI-IV. Geometry of a Rhodium Complex with Two Z-Type Ligands

Z-type ligands do not affect the d electron count of transition metal centres. Therefore, the tetrahedral geometry of Rh1 centre of complex **2** does not necessarily support the Rh(−I) character of Rh1 centre. To explain the geometry around Rh1 centre, the structure of a model ML_2Z_2-type Rh(−I) complex, $[Rh(PMe_3)_2(BMe_3)_2]^-$, was calculated. The model complex $[Rh(PMe_3)_2(BMe_3)_2]^-$ exhibited distorted tetrahedral geometry (Figure S12), which resembles the geometry around Rh1 centre in complex **2**, as discussed in the main text. $[Rh(PMe_3)_2(BMe_3)_2]^-$ favours this geometry, possibly because the bending of the $Rh(PMe_3)_2$ fragment maximizes the overlap between d-orbitals of the Rh centre and vacant orbitals of the borane ligands (Figure S13).

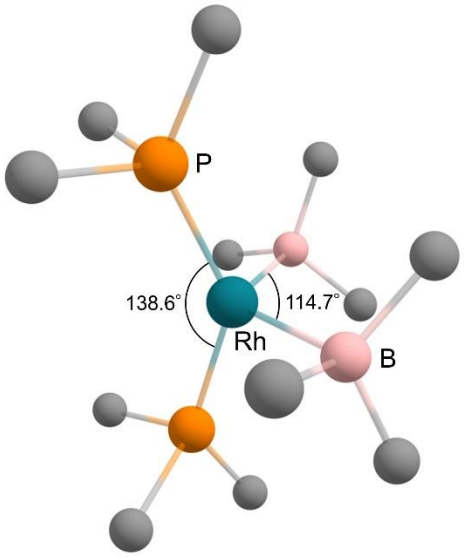

Figure S12. Computed structure of $[Rh(PMe_3)_2(BMe_3)_2]^-$ (τ_4 = 0.76)

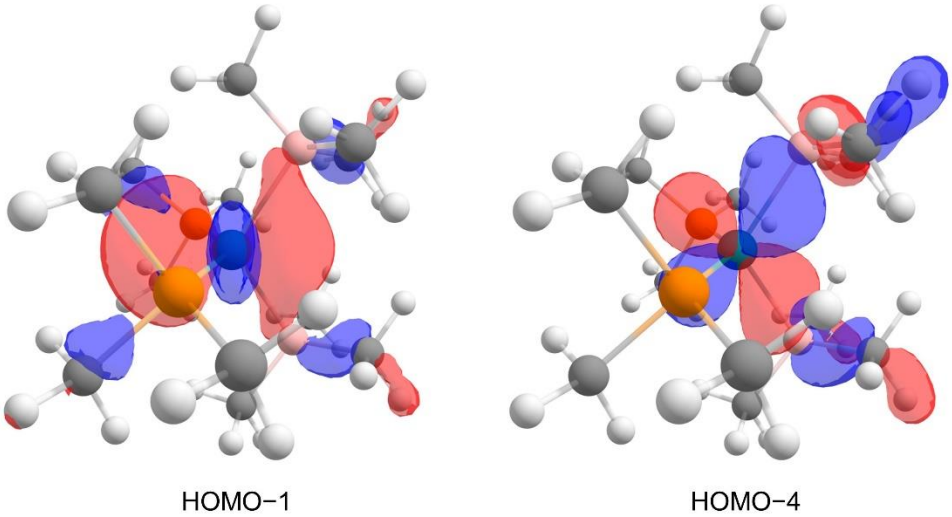

Figure S13. Frontier orbitals of $[Rh(PMe_3)_2(BMe_3)_2]^-$ stabilized by the bending of the $Rh(PMe_3)_2$ fragment.

VII. References

1 A. B. Pangborn, M. A. Giardello, R. H. Grubbs, R. K. Rosen and F. J. Timmers, *Organometallics*, 1996, **15**, 1518–1520.

2 K. Masada, S. Kusumoto and K. Nozaki, *Organometallics*, 2023, **42**, 971–981.

3 H. Kameo, Y. Hashimoto and H. Nakazawa, *Organometallics*, 2012, **31**, 3155–3162.

4 K. Masada, S. Kusumoto and K. Nozaki, *Angew. Chem. Int. Ed.*, 2022, **61**, e202117096.

5 O. V. Dolomanov, L. J. Bourhis, R. J. Gildea, J. A. K. Howard and H. Puschmann, *J. Appl. Crystallogr.*, 2009, **42**, 339–341.

6 G. M. Sheldrick, *University of Göttingen. Germany*.

7 G. M. Sheldrick, *University of Göttingen. Germany*.

8 M. J. Frisch, G. W. Trucks, H. B. Schlegel, G. E. Scuseria, M. A. Robb, J. R. Cheeseman, G. Scalmani, V. Barone, G. A. Petersson, H. Nakatsuji, X. Li, M. Caricato, A. V. Marenich, J. Bloino, B. G. Janesko, R. Gomperts, B. Mennucci, H. P. Hratchian, J. V. Ortiz, A. F. Izmaylov, J. L. Sonnenberg, Williams, F. Ding, F. Lipparini, F. Egidi, J. Goings, B. Peng, A. Petrone, T. Henderson, D. Ranasinghe, V. G. Zakrzewski, J. Gao, N. Rega, G. Zheng, W. Liang, M. Hada, M. Ehara, K. Toyota, R. Fukuda, J. Hasegawa, M. Ishida, T. Nakajima, Y. Honda, O. Kitao, H. Nakai, T. Vreven, K. Throssell, J. A. Montgomery Jr, J. E. Peralta, F. Ogliaro, M. J. Bearpark, J. J. Heyd, E. N. Brothers, K. N. Kudin, V. N. Staroverov, T. A. Keith, R. Kobayashi, J. Normand, K. Raghavachari, A. P. Rendell, J. C. Burant, S. S. Iyengar, J. Tomasi, M. Cossi, J. M. Millam, M. Klene, C. Adamo, R. Cammi, J. W. Ochterski, R. L. Martin, K. Morokuma, O. Farkas, J. B. Foresman and D. J. Fox, *Gaussian 16 Rev. C.03*, Wallingford, CT, 2016.

9 J. P. Perdew, M. Ernzerhof and K. Burke, *J. Chem. Phys.*, 1996, **105**, 9982–9985.

10 F. Weigend and R. Ahlrichs, *Phys. Chem. Chem. Phys.*, 2005, **7**, 3297–3305.

11 F. Weigend, *Phys. Chem. Chem. Phys.*, 2006, **8**, 1057–1065.

12 S. Grimme, J. Antony, S. Ehrlich and H. Krieg, *J. Chem. Phys.*, 2010, **132**, 154104.

13 J.-D. Chai and M. Head-Gordon, *Phys. Chem. Chem. Phys.*, 2008, **10**, 6615–6620.